

# Time-optimal universal quantum gates on superconducting circuits

Ze Li,<sup>1</sup> Ming-Jie Liang,<sup>1</sup> and Zheng-Yuan Xue<sup>1,2,\*</sup>

<sup>1</sup>Guangdong Provincial Key Laboratory of Quantum Engineering and Quantum Materials, and School of Physics and Telecommunication Engineering, South China Normal University, Guangzhou 510006, China

<sup>2</sup>Guangdong-Hong Kong Joint Laboratory of Quantum Matter, and Frontier Research Institute for Physics, South China Normal University, Guangzhou 510006, China

(Dated: January 10, 2023)

Decoherence is an inevitable problem when targeting to increase the fidelity of quantum gates, and thus is one of the main obstacles for large-scale quantum computation. The longer a gate operation is, the more decoherence-induced gate infidelity will be. Therefore, how to shorten the gate time becomes an urgent problem to be solved. To this end, time-optimal control based on solving the quantum brachistochron equation is a straightforward solution. Here, based on time-optimal control, we propose a scheme to realize universal quantum gates on superconducting qubits, in a two-dimensional square lattice configuration, and the two-qubit gate fidelity can be higher than 99.7%. Meanwhile, we can further accelerate the z-axis gate considerably by adjusting the time-independent detuning. Finally, in order to reduce the influence of the dephasing error, decoherence free subspace is also incorporated in our physical implementation. Therefore, we present a promising fast scheme for large-scale quantum computation.

## I. INTRODUCTION

Due to the intrinsic superposition nature, quantum computation can not only greatly shorten the calculation time of certain problems, but also deal with some hard problems that are hard for classical computers. Recently, quantum computation has been implemented in a variety of systems [1–4], among which, the superconducting quantum circuits system is one of the most promising candidates [5–9]. However, besides the existence of operational errors, a quantum system will inevitably couple to its surrounding environment, and thus lead to an increase in the distortion of quantum states or operations. Therefore, how to achieve high fidelity quantum gates in quantum systems is an urgent problem to be solved.

In the presence of noise, precise quantum control can be realized by the fastest possible evolution. Therefore, finding a shorter gate evolution path to shorten the gate-time has become an effective means to achieve high fidelity quantum gates. Time-optimal control (TOC) based on solving the quantum brachistochrone equation (QBE) [10] is an effective scheme to shorten the evolution time [11]. Recently, TOC based schemes for unitary operations have been proposed [11–17] and experimental demonstrated [18–23], where the needed time for specific quantum gate operations has been reduced significantly. However, universal quantum control with analytical solution can only be possible for specific cases [12].

Here, based on TOC, we propose a scheme to realize universal quantum gates on superconducting transmon qubits, arranged in a two-dimensional (2D) square lattice configuration, which is capable for large-scale universal quantum computation. In our scheme, controlling the time-dependent frequency of the qubits, we can achieve the tunable coupling between two transmon qubits [24, 25]. Meanwhile, we can further shorten the evolution time of the  $Z$ -axis gate by adjusting the time-independent detuning. Furthermore, to eliminate the ef-

fect of dephasing, which is another important factor affecting the quantum gate fidelity, decoherence-free subspaces (DFS) encoding [26–28] has been incorporated and the robustness of our gates with respect to the decoherence is presented. Therefore, our work realized high fidelity universal quantum gate on superconducting circuits, which is a promising alternation for future large-scale quantum computation.

## II. THE GENERAL THEORY

For a general two-level system, denoted by  $\{|0\rangle = (1, 0)^\dagger, |1\rangle = (0, 1)^\dagger\}$ , assuming  $\hbar = 1$  hereafter, when under the driving of an external field, its general interaction Hamiltonian is

$$\mathcal{H}(t) = \frac{1}{2} \begin{pmatrix} \delta(t) & \Omega(t)e^{-i\phi(t)} \\ \Omega(t)e^{i\phi(t)} & -\delta(t) \end{pmatrix}, \quad (1)$$

where  $\Omega(t)$  and  $\phi(t)$  is the time-dependent coupling strength and phase of the driving field,  $\delta(t)$  is the time-dependent detuning between the qubit frequency and the driving field frequency. Assuming there are two mutually orthogonal evolution states  $|\Psi_\pm(t)\rangle$  that satisfy the time-dependent Schrödinger equation of Hamiltonian in Eq. (1). The evolution operator can be written as

$$U(t) = \mathbf{T}e^{i\int \mathcal{H}(t)dt} = |\Psi_+(t)\rangle \langle\Psi_+(0)| + |\Psi_-(t)\rangle \langle\Psi_-(0)|, \quad (2)$$

where  $\mathbf{T}$  is the time-ordering operator. In order to construct a particular evolution operator, we need to define a set of auxiliary basis vectors  $|\psi_\pm(t)\rangle = e^{-i\gamma_\pm(t)} |\Psi_\pm(t)\rangle$  with  $\gamma_\pm(0) = 0$  and  $\gamma_+(t) = -\gamma_-(t)$ , which satisfy the boundary condition of  $|\psi_\pm(\tau)\rangle = |\psi_\pm(0)\rangle = |\Psi_\pm(0)\rangle$ . We select a pair of dressed states

$$\begin{aligned} |\psi_+(t)\rangle &= \cos \frac{\chi(t)}{2} |0\rangle + \sin \frac{\chi(t)}{2} e^{i\xi(t)} |1\rangle, \\ |\psi_-(t)\rangle &= \sin \frac{\chi(t)}{2} e^{-i\xi(t)} |0\rangle - \cos \frac{\chi(t)}{2} |1\rangle, \end{aligned} \quad (3)$$

\* zyxue83@163.com

as a set of auxiliary basis vectors, which are the eigenstates of the Lewis-Riesenfeld invariant [29] of Eq. (1),

$$I(t) = \frac{\mu}{2} \begin{pmatrix} \cos \chi(t) & \sin \chi(t) e^{-i\xi(t)} \\ \sin \chi(t) e^{i\xi(t)} & -\cos \chi(t) \end{pmatrix}, \quad (4)$$

where  $\mu$  is an arbitrary constant. The auxiliary basis vectors  $|\psi_{\pm}(t)\rangle$  shows their evolutionary details on the Bloch sphere through the time-dependent parameters  $\xi(t)$  and  $\chi(t)$ .

Then, by solving dynamic invariant equation of  $i\partial I(t)/\partial t - [\mathcal{H}(t), I(t)] = 0$ , the parameter  $\{\xi(t), \chi(t)\}$  of  $|\psi_{\pm}(t)\rangle$  are decided by the parameters  $\{\Omega(t), \phi(t), \delta(t)\}$  of the Hamiltonian in Eq. (1) as [29–31]

$$\begin{aligned} \dot{\xi}(t) &= \delta(t) - \Omega(t) \cot \chi(t) \cos[\phi(t) - \xi(t)], \\ \dot{\chi}(t) &= \Omega(t) \sin[\phi(t) - \xi(t)]. \end{aligned} \quad (5)$$

After an evolution time  $\tau$ , by solving the Schrödinger equation  $\mathcal{H}(t) |\Psi_{\pm}(t)\rangle = i\hbar \frac{\partial}{\partial t} |\Psi_{\pm}(t)\rangle$ , we can obtain the overall phase as

$$\gamma(\tau) = \int_0^{\tau} \frac{2\dot{\xi}(t) \sin^2[\chi(t)/2] - \delta(t)}{2 \cos \chi(t)} dt. \quad (6)$$

By setting  $\chi(t)$  to be a constant, we can get a general evolution operator of the process as

$$U(\tau) = \cos \gamma' \begin{pmatrix} e^{-i\xi_-} & 0 \\ 0 & e^{i\xi_-} \end{pmatrix} + i \sin \gamma' \begin{pmatrix} \cos \chi e^{-i\xi_-} & \sin \chi e^{-i\xi_+} \\ \sin \chi e^{i\xi_+} & -\cos \chi e^{i\xi_-} \end{pmatrix}, \quad (7)$$

where  $\gamma' = \gamma(\tau) + \xi_-$  and  $\xi_{\pm} = [\xi(\tau) - \xi(0)]/2$ . We can get the appropriate parameters  $\gamma$ ,  $\chi$  and  $\xi(t)$  to construct target quantum gates by controlling the coupling strength  $\Omega(t)$  and the phase  $\phi(t)$ .

For realistic physical implementation, the interaction term in Eq. (1),  $\mathcal{H}_c(t) = \Omega(t) [\cos \phi(t) \sigma_x + \sin \phi(t) \sigma_y] / 2$ , needs to satisfy the following two conditions. Firstly, the coupling strength is limited, here we set the maximum of  $\Omega(t)$  as  $\Omega = [\Omega(t)]_{max}$ , that is, we need to satisfy  $f_1(\mathcal{H}_c(t)) = [Tr(\mathcal{H}_c(t))^2 - \Omega^2/2]/2 = 0$ . Then, the form of the interaction Hamiltonian is usually not arbitrary. Here, independent  $\sigma_z$  operator can't be achieved, so it is necessary to satisfy  $f_2(\mathcal{H}_c(t)) = Tr(\mathcal{H}_c(t) \sigma_z) = 0$ . Considering the these two conditions, based on the QBE of

$$\frac{dF}{dt} = -i[\mathcal{H}(t), F], \quad (8)$$

where

$$\begin{aligned} F &= \frac{\partial L_C}{\partial \mathcal{H}_c(t)} = \frac{\partial (\sum_{j=1,2} \lambda_j f_j(\mathcal{H}_c(t)))}{\partial \mathcal{H}_c(t)} \\ &= \lambda_1 \mathcal{H}_c(t) + \lambda_2 \sigma_z, \end{aligned} \quad (9)$$

and Lagrange multiplier  $\lambda_j$  is defined as  $\lambda_1 = 1/\Omega$  and  $\lambda_2 = -c/2$ , we can obtain  $\phi(t) = \phi_0 + \phi'(t)$ ,  $\phi'(t) = \int_0^t [c\Omega + \delta] dt' = \eta t$ , where  $\eta$  and  $c$  are the constant. Finally, in order to implement TOC based quantum operations,

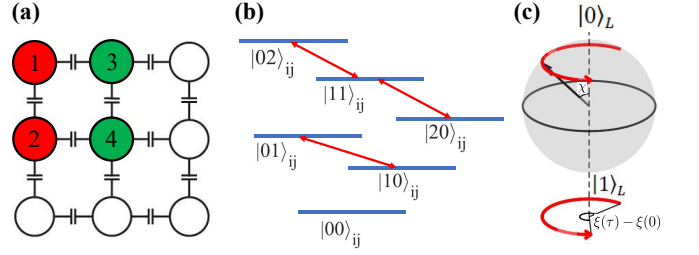


FIG. 1. Illustration of our proposed scheme. (a) A scalable 2D square lattice consists of transmon qubits, where adjacent qubits are capacitively coupled. Two physical qubits of the same color encoded as a DFS logical qubit. (b) The energy levels of two adjacent coupled qubits  $T_i$  and  $T_j$ , where different excitation subspaces can be used to implement different quantum gate. (c) Illustration of the evolution path of the TOC based scheme (red line) on the Bloch sphere, where  $\chi$  is the angle between the direction of the auxiliary basis vector and the vertical axis, and  $\xi(\tau) - \xi(0)$  is the horizontal angle shift of the auxiliary basis vector at a specific time  $\tau$ .

the coupling strength, detuning and phase need to satisfy conditions of  $\Omega = 0$ ,  $\delta = 0$  and  $\phi = \eta$ , respectively.

Now, we calculated the gate operation time  $\tau$  by solving the Eq. (5) and Eq. (6). The gate time of  $H$ ,  $S$ , and  $T$  gates can be expressed as

$$\begin{aligned} \tau_H &= \frac{\sqrt{2}\pi}{2\Omega}, \\ \tau_S &= \frac{\pi}{2(\Omega^2 + \delta^2)} \left( \sqrt{16\delta^2 + 7\Omega^2} - 3\delta \right), \\ \tau_T &= \frac{\pi}{4(\Omega^2 + \delta^2)} \left( \sqrt{64\delta^2 + 15\Omega^2} - 7\delta \right), \end{aligned} \quad (10)$$

which indicate that  $\delta$  can be adjusted to further accelerate the  $S$  and  $T$  gates, due to the extra freedom on  $\chi$ .

### III. PHYSICAL IMPLEMENTATION

Here, in this section, we implemented our TOC-based scheme in the 2D square superconducting qubit lattice, as shown in Fig. 1(a), where the coupling strength between two adjacent transmons is fixed.

#### A. Parametric Tunable Coupling

In order to control single-logical-qubit units and two-logical-qubits units independently and construct the targeted quantum gates exactly, tunable interactions between any two transmon qubits should be implemented. For two adjacent transmon qubits  $T_i$  and  $T_j$ , the interaction Hamiltonian can be expressed as

$$\begin{aligned} \mathcal{H}_{ij}^0 &= \sum_{k=i,j} [\omega_k |1\rangle_k \langle 1| + (2\omega_k - \alpha_k) |2\rangle_k \langle 2|] \\ &+ g_{ij} (|10\rangle_{ij} \langle 01| + \sqrt{2} |11\rangle_{ij} \langle 02| + \sqrt{2} |20\rangle_{ij} \langle 11| + \text{H.c.}), \end{aligned} \quad (11)$$

where  $\omega_{i,j}$  and  $\alpha_{i,j}$  are the frequency and anharmonicity of the  $i,j$ -th transmon qubit  $T_i$  and  $T_j$ , respectively,  $|\text{CD}\rangle_{ij} = |C\rangle_i \otimes |D\rangle_j$ . To achieve tunable coupling between  $T_i$  and  $T_j$ , we added a frequency modulation in the form of  $\omega_j = \omega_{j0} + \epsilon_j \cos[\nu_j t + \phi_j(t)]$  for qubit  $T_j$ , with the driving frequency and phase being  $\nu_j$  and  $\phi_j(t)$ , respectively. Meanwhile, frequency of  $T_i$  is fixed, which is written as  $\omega_i = \omega_{i0}$  for the same layout as  $\omega_j$ . Moving into the interaction picture with respect to

$$U_{ij}^I = U_i^I \times U_j^I, \quad (12)$$

with

$$U_i^I = \exp[-i(\omega_{i0} b_i^\dagger b_i - \frac{\alpha_i}{2} b_i^\dagger b_i^\dagger b_i b_i) t], \quad (13)$$

$$U_j^I = \exp\{-i[\omega_{j0} t + \Gamma_j \sin(\nu_j t + \phi_j(t))] b_j^\dagger b_j - \frac{\alpha_j}{2} b_j^\dagger b_j^\dagger b_j b_j t\}, \quad (14)$$

with  $b_{i,j} = (|0\rangle_{i,j} \langle 1| + \sqrt{2}|1\rangle_{i,j} \langle 2|)$ ,  $\Gamma_j = \epsilon_j / [\nu_j + \dot{\phi}_j(t)]$ , and then using Jacobi-Anger identity,  $\exp(-i\Gamma \sin \theta) = \sum_n J_n(\Gamma) \exp(-in\theta)$ , with  $J_n$  is the  $n$ -th Bessel function, the transformed Hamiltonian can be written as

$$\begin{aligned} \mathcal{H}_{ij}^I &= g_{ij} e^{i\Delta_{ij}} \sum_{n=-\infty}^{+\infty} J_n(\Gamma_j) e^{-in(\nu_j t + \phi_j(t))} \{|10\rangle_{ij} \langle 01| \\ &+ \sqrt{2} e^{i\alpha_j t} |11\rangle_{ij} \langle 02| \\ &+ \sqrt{2} e^{-i\alpha_j t} |20\rangle_{ij} \langle 11|\} + \text{H.c.}, \end{aligned} \quad (15)$$

where  $\Delta_{ij} = -\Delta_{ji} = \omega_{i0} - \omega_{j0}$  is the frequency difference between  $T_i$  and  $T_j$ . The energy level diagram is shown in Fig. 1(b), in which any two adjacent levels can be used to realize quantum computation. In addition,  $\Gamma_j$  can be tuned to achieve adjustable coupling between  $T_i$  and  $T_j$ , then we can select appropriate parameters of the modulation filed to construct target quantum gates.

## B. Single-Logical-Qubit gate based on TOC

In order to decrease dephasing which is a type of the decoherence, the DFS encoding can be incorporated in our scheme. Set two adjacent transmon qubits in Eq. (15) to be qubits  $T_1$  and  $T_2$  as shown in Fig. 1(a), where the logical qubits  $\{|0\rangle_L, |1\rangle_L\}$  can be encoded in their single excitation subspace, i.e.,  $S_1 = \text{Span}\{|0\rangle_L = |10\rangle_{12}, |1\rangle_L = |01\rangle_{12}\}$ . In order to obtain a Hamiltonian in the form of Eq. (1) for constructing universal quantum gates. It is natural to go into the rotating frame with respect to

$$U_A = \exp\left[i\frac{\delta}{2} t (|0\rangle_L \langle 0| - |1\rangle_L \langle 1|)\right], \quad (16)$$

the transformed Hamiltonian of Eq. (15) can be written as

$$\begin{aligned} \mathcal{H}'_{12} &= \frac{\delta}{2} (|0\rangle_L \langle 0| - |1\rangle_L \langle 1|), \\ &+ g_{12} [\mathcal{K}_{12} e^{i(\Delta_{12} - \delta)t} |0\rangle_L \langle 1| + \text{H.c.}] \end{aligned} \quad (17)$$

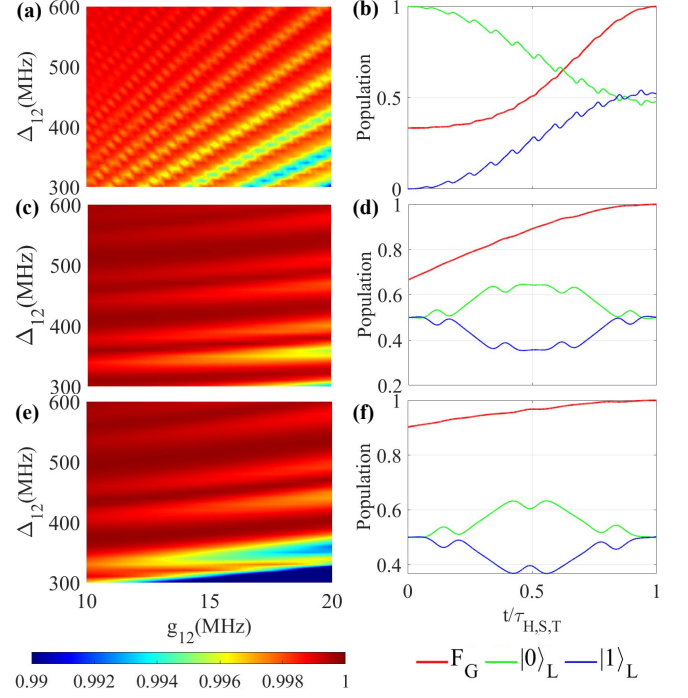


FIG. 2. The gate fidelity as a function of the qubits' frequency differences  $\Delta_{12}$  and the coupling strength  $g_{12}$ . The numerical result of  $H$ ,  $S$  and  $T$  gates are shown in (a), (c) and (e), respectively. The dynamics of the state population and fidelity of  $H$ ,  $S$  and  $T$  gates are shown in (b), (d) and (f), respectively.

where  $\mathcal{K}_{12} = \sum_{n=-\infty}^{+\infty} J_n(\Gamma_2) \exp\{-in(\nu_2 t + \phi_2)\}$ . Choose the modulating frequency to meet  $\nu_2 = \Delta_{12} - \delta$  in Eq. (17), after the rotational wave approximation, we obtain the Hamiltonian in the logical basis  $S_1$  as

$$\mathcal{H}_{12}^{\text{eff}} = \frac{1}{2} \begin{pmatrix} \delta & \Omega e^{-i\phi_2} \\ \Omega e^{i\phi_2} & -\delta \end{pmatrix}, \quad (18)$$

where  $\Omega = 2g_{12}J_1(\Gamma_2)$ . Therefore, according to the general theory in the last section, we can use TOC based scheme to construct arbitrary single-logical-qubit quantum gates. We set different parameters of the physical qubits for  $H$ ,  $S$  and  $T$  gates. For  $H$  gate, which is correspond to  $\gamma'_H = \frac{\pi}{2}$ ,  $\xi_H^+ = \xi_H^- = \pi$  and  $\chi_H = \frac{\pi}{4}$ . For  $S$  and  $T$  gates, which is correspond to  $\gamma'_S = \gamma'_T = \pi$ ,  $\xi_S^- = -3\pi/4$  and  $\xi_T^- = -7\pi/8$ . Based on TOC and solving Eq. (15), here,  $\xi(t)$  is in the form of a linear function and  $\chi$  is a constant, whose path in Bloch sphere is intuitive shown in Fig. 1(c).

Next, we use the Lindblad master equation of

$$\dot{\rho} = -i[\mathcal{H}(t), \rho] + \frac{r_-}{2} \mathcal{A}(b_-) + \frac{r_z}{2} \mathcal{A}(b_z), \quad (19)$$

to simulate the performance of our scheme for the single-logical-qubit gates, where  $\rho$  is density operator of the quantum system,  $\mathcal{A}(b) = 2b\rho b^\dagger - \rho b^\dagger b - b^\dagger b\rho$  is the Lindblad operator,  $r_-^1 = r_-^2 = r_-$  and  $r_z^1 = r_z^2 = r_z$  are the decay and dephasing rates of the two transmons qubits  $T_1$  and  $T_2$ , respectively, with  $b_- = \sum_{k=1,2} (|0\rangle_k \langle 1| + \sqrt{2}|1\rangle_k \langle 2|)$  and  $b_z =$

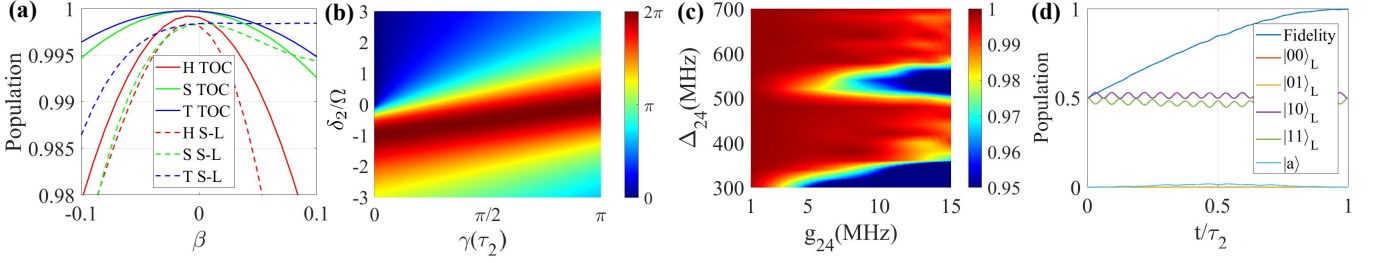


FIG. 3. (a) Comparative results for the gate robustness. Frequency drift error of TOC based (solid line) and S-L based gates (dot line). (b) The operation time  $\tau_2$  in unit of  $1/\Omega$  with respect to the rotation angle  $\gamma(\tau_2)$  and  $\delta_2/\Omega$ . (c) State fidelity as the function of the qubits frequency differences  $\Delta_{24}$  and capacitive coupling strength  $g_{24}$ . (d) Considering the adjacent interactions from  $T_1$  and  $T_3$ , state population and fidelity dynamics of the CP-gate process with prescribed parameters as presented in the maintext.

$\sum_{k=1,2} (|1\rangle_k \langle 1| + 2|2\rangle_k \langle 2|)$ . Setting  $r = r_- = r_z = 2\pi \times 4$  kHz [8], as shown in Fig. 2, taking  $g_{12}$  and  $\Delta_{12}$  as variables, we numerically obtain the fidelity of the  $H$ ,  $S$  and  $T$  gates, which are defined as  $F = \text{Tr}(U^\dagger U')/\text{Tr}(U^\dagger U)$ , where  $U'$  represents the evolution matrix under decoherence. For typical examples, we consider the parameters of the physical qubits as follow. The qubit frequency difference  $\Delta_{12} = 2\pi \times 520$  MHz, the capacitive coupling strength  $g_{12} = 2\pi \times 14.5$  MHz, the detuning of  $H$ ,  $S$  and  $T$  gates are modulated to  $\delta_H = 2\pi \times 29.58$  MHz,  $\delta_S = 2\pi \times 25$  MHz,  $\delta_T = 2\pi \times 15$  MHz,  $\Gamma_2$  is set as 1.5, and  $\Omega = 2\pi \times 16.18$  MHz. With those settings, fidelities of the  $H$ ,  $S$ , and  $T$  gates can reach  $F_H=99.89\%$ ,  $F_S=99.97\%$ , and  $F_T=99.97\%$ , respectively.

Next, to test the gate robustness of our scheme, we consider the frequency drift error of the two transmons qubits  $T_1$  and  $T_2$ , which is the main error source of the superconducting qubit lattice and is in the form of  $\omega_{1,\beta} = \omega_1 + \beta\Omega$  and  $\omega_{2,\beta} = \omega_2 - \beta\Omega$ . Under the interaction picture, the interaction Hamiltonian with error can be expressed as

$$\mathcal{H}'_{12,\beta} = \mathcal{H}_{12}^I + \beta\Omega (b_1^+ b_1 - b_2^+ b_2) \quad (20)$$

As shown in Fig. 3(a), we found that under the effect of qubit frequency drift, our scheme exhibits a better resistance than the single-loop (S-L) based gate scheme [32].

### C. Two-Logical-Qubit gate based on TOC

We next consider the implementation of the controlled phase gate (CP-gate), which is an important element for the universal quantum gates. As shown in Fig. 1(a), we consider a two-logical qubits unit with two pairs of transmon qubits,  $T_1$  and  $T_2, T_3$  and  $T_4$ . Assuming  $|\text{CDEF}\rangle = |\text{C}\rangle_i \otimes |\text{D}\rangle_j \otimes |\text{E}\rangle_k \otimes |\text{F}\rangle_l$ , there exists a four-dimensional DFS  $S_2 = \text{Span}\{|00\rangle_L = |1010\rangle, |01\rangle_L = |1001\rangle, |10\rangle_L = |0110\rangle, |11\rangle_L = |0101\rangle\}$ . In addition, an auxiliary state  $|a\rangle = |0200\rangle$  is needed to assist the implementation of the CP-gate. We consider the interaction between two adjacent physical qubits  $T_2$  and  $T_4$ . Similar to the single-logical-qubit case, frequency of the  $T_2$  qubit  $\omega_2$  needs to be modulated as  $\omega_2 = \omega_{20} + \epsilon_2 \cos(\nu_2 t + \phi_2)$  to achieve tunable coupling between qubits  $T_2$  and  $T_4$ , in the subspace of  $\{|a\rangle, |11\rangle_L\}$ , the interacting Hamiltonian can be

written as

$$\mathcal{H}'_{42} = \frac{\delta}{2} (|a\rangle\langle a| - |11\rangle_L \langle 11|) + [\sqrt{2}g_{42}\mathcal{K}_{42}e^{i(\Delta_{42}+\alpha_2+\delta)t}|11\rangle_L \langle a| + \text{H.c.}], \quad (21)$$

where  $\mathcal{K}_{42} = \sum_{n=-\infty}^{+\infty} J_n(\Gamma'_2) \exp[-in(\nu_2 t + \phi_2)]$ . When we choose the resonance frequency  $\nu_2 = \Delta_{24} - \alpha_2 - \delta_2$ , see Eq. (15), assume  $\Omega = 2g_{42}J_1(\Gamma_2)$ ,  $\Gamma'_2 = 1.6$  and  $\phi = \phi_2 + \pi$ , then the Hamiltonian in Eq. (21) reduces to

$$\mathcal{H}_{42}^{\text{eff}} = \frac{1}{2} \begin{pmatrix} \delta & \Omega e^{-i\phi} \\ \Omega e^{i\phi} & -\delta \end{pmatrix}, \quad (22)$$

where  $|a\rangle$  and  $|11\rangle_L$  form the set of orthogonal basis vectors, and  $\phi_2 = \eta t$  is a linear function according to TOC solution. The evolution operator is shown in Eq. (7). When we set  $\gamma' = \pi$ , we can obtain the evolution operator in the subspace  $S_2$  as

$$U(\tau_2) = \begin{pmatrix} 1 & 0 & 0 & 0 \\ 0 & 1 & 0 & 0 \\ 0 & 0 & 1 & 0 \\ 0 & 0 & 0 & e^{i\gamma(\tau_2)} \end{pmatrix}, \quad (23)$$

where  $\gamma(\tau_2) = \xi_2^- + \pi$ . In this way, the CP gate can be obtained. The gate time can be solved as

$$\tau_2 = \frac{2}{\Omega^2 + \delta^2} \{ \delta[\gamma(\tau_2) - \pi] + \sqrt{\pi^2 \delta^2 - \Omega^2 [\gamma(\tau_2)^2 - 2\pi\gamma(\tau_2)]} \}. \quad (24)$$

Similar to the  $S$  and  $T$  gates, the detuning  $\delta_2$  can also be used to further accelerate the gate time, as shown in Fig. 3(b), where we have set  $\gamma(\tau_2) = \pi/2$ ,  $\delta_2 = 2\pi \times 27$  MHz and  $\delta_2/\Omega = 2.3929$ .

In order to properly evaluate the performance of the CP-gate, with the initial state  $|\psi_{in}\rangle = (|10\rangle_L + |11\rangle_L)/\sqrt{2}$ , the effect of frequency difference  $\Delta_{24}$  and coupling strength  $g_{12}$  on the gate fidelity is shown in Fig. 3(c). When the parameters are set as  $\Delta_{24} = 2\pi \times 600$  MHz,  $g_{24} = 2\pi \times 7$  MHz,  $\alpha_2 = 2\pi \times 210$  MHz and  $\alpha_4 = 2\pi \times 230$  MHz, the fidelity of CP-gate can reach 99.88%. Actually, the leakage about two adjacent qubits  $T_1$  and  $T_3$  should be considered as well, when we set  $\Delta_{12} = \Delta_{34} = 2\pi \times 900$  MHz,

$\alpha_1 = 2\pi \times 200$  MHz,  $\alpha_3 = 2\pi \times 220$  MHz, the fidelity of  $CP$  gate can reach 99.72%. The state evolution process is shown in Fig. 3(d), Lindblad master equation in Eq. (19) should be considered as  $b_- = \sum_{k=1}^4 (|0\rangle_k \langle 1| + \sqrt{2}|1\rangle_k \langle 2|)$ ,  $b_z = \sum_{k=1}^4 (|1\rangle_k \langle 1| + 2|2\rangle_k \langle 2|)$ , and the rates of decay and dephasing for each transmon qubit is set as  $r = r_-^k = r_z^k = 2\pi \times 4$  kHz.

#### IV. CONCLUSION

In conclusion, we propose a scheme with TOC combined with DFS, and implement a universal quantum gate set on

superconducting transmon qubits. For  $S$ ,  $T$  and  $CP$  gates, by adjusting the detuning, the gate operations can be completed in an extremely short time. Thus, our scheme provides a promising way towards the practical realization of fast quantum gates.

#### ACKNOWLEDGMENTS

This work was supported by the Key-Area Research and Development Program of Guangdong Province (Grant No. 2018B030326001), the National Natural Science Foundation of China (Grant No. 12275090), and Guangdong Provincial Key Laboratory (Grant No. 2020B1212060066).

- 
- [1] J. I. Cirac and P. Zoller, *Phys. Rev. Lett.* **74**, 4091 (1995).  
 [2] Q. A. Turchette, C. J. Hood and W. Lange, *Phys. Rev. Lett.* **75**, 4710 (1995).  
 [3] G. K. Brennen, C. M. Caves and P. S. Jessen, *Phys. Rev. Lett.* **82**, 1060 (1999).  
 [4] D. Jaksch, H. J. Briegel and J. I. Cirac, *Phys. Rev. Lett.* **82**, 1975 (1999).  
 [5] Y. Makhlin, G. Schön and A. Shnirman, *Rev. Mod. Phys.* **73**, 357 (2001).  
 [6] J. Clarke and F. K. Wilhelm, *Nature* **453**, 1031 (2008).  
 [7] J. Q. You and F. Nori, *Nature* **474**, 589 (2011).  
 [8] M. H. Devoret and R. J. Schoelkopf, *Science* **339**, 1169 (2013).  
 [9] X. Gu, A. F. Kockum and A. Miranowicz, *Phys. Rep.* **718**, 1102 (2017).  
 [10] H. J. Sussmann and J. C. Willems, *IEEE Control Syst. Mag.* **17**, 32 (1997).  
 [11] A. Carlini, A. Hosoya, T. Koike, and Y. Okudaira, *Phys. Rev. Lett.* **96**, 060503 (2006).  
 [12] A. Carlini and T. Koike, *J. Phys. A.* **46**, 045307 (2013).  
 [13] X.-T. Wang, M. Allegra, K. Jacobs, S. Lloyd, C. Lupo, and M. Mohseni, *Phys. Rev. Lett.* **114**, 170501 (2015).  
 [14] T. Chen and Z.-Y. Xue, *Phys. Rev. Appl.* **14**, 064009 (2020).  
 [15] T. Chen, P. Shen and Z.-Y. Xue, *Phys. Rev. Appl.* **14**, 034038 (2020).  
 [16] B.-J. Liu, Z.-Y. Xue, and M.-H. Yung, arXiv:2001.05182.  
 [17] G. O. Alves and E. Sjöqvist, *Phys. Rev. A* **106**, 032406 (2022).  
 [18] M. Lapert, Y. Zhang, M. Braun, S. J. Glaser, and D. Sugny, *Phys. Rev. Lett.* **104**, 083001 (2010).  
 [19] M. G. Bason, M. Viteau, N. Malossi, P. Huillery, E. Arimondo, D. Ciampini, R. Fazio, V. Giovannetti, R. Mannella, and O. Morsch, *Nat. Phys.* **8**, 147 (2012).  
 [20] C. Avinadav, R. Fischer, P. London, and D. Gershoni, *Phys. Rev. B* **89**, 245311 (2014).  
 [21] J. Geng, Y. Wu, X.-T. Wang, K. Xu, F. Shi, Y. Xie, X. Rong, and J. Du, *Phys. Rev. Lett.* **117**, 170501 (2016).  
 [22] Z. Han, Y. Dong, B. Liu, X. Yang, S. Song, L. Qiu, D. Li, J. Chu, W. Zheng, J. Xu, T. Huang, Z. Wang, X. Yu, X. Tan, D. Lan, M.-H. Yung, and Y. Yu arXiv:2004.10364  
 [23] Y. Dong, C. Feng, Y. Zheng, X.-D. Chen, G.-C. Guo, and F.-W. Sun, *Phys. Rev. Res.* **3**, 043177 (2021).  
 [24] X. Li, Y. Ma, J. Han, T. Chen, Y. Xu, W. Cai, H. Wang, Y. P. Song, Z.-Y. Xue, Z.-Q. Yin, and L. Sun, *Phys. Rev. Appl.* **10**, 054009 (2018).  
 [25] J. Chu, D. Li, X. Yang, S. Song, Z. Han, Z. Yang, Y. Dong, W. Zheng, Z. Wang, X. Yu, D. Lan, X. Tan, and Y. Yu, *Phys. Rev. Appl.* **13**, 064012 (2020).  
 [26] L.-M. Duan and G.-C. Guo, *Phys. Rev. Lett.* **79**, 1953 (1997).  
 [27] P. Zanardi and M. Rasetti, *Phys. Rev. Lett.* **79**, 3306 (1997).  
 [28] D. A. Lidar, I. L. Chuang, and K. B. Whaley, *Phys. Rev. Lett.* **81**, 2594 (1998).  
 [29] H. R. Lewis and W. B. Riesenfeld, *J. Math. Phys.* **10**, 1458 (1969).  
 [30] X. Chen, E. Torrontegui, and J. G. Muga, *Phys. Rev. A.* **83**, 062116 (2011).  
 [31] A. Ruschhaupt, X. Chen, D. Alonso, and J. G. Muga, *New J. Phys.* **14**, 093040 (2012).  
 [32] T. Chen and Z.-Y. Xue, *Phys. Rev. Appl.* **10**, 054051 (2018).